

# The constructive role of diversity on the global response of coupled neuron systems

Toni Pérez<sup>1</sup>, Claudio R. Mirasso<sup>2</sup>, Raúl Toral<sup>2</sup> and James D. Gunton<sup>1</sup>

<sup>1</sup>*Department of Physics, Lehigh University, Bethlehem, Pennsylvania 18015, USA*

<sup>2</sup>*IFISC (Instituto de Física Interdisciplinar y Sistemas Complejos),*

*UIB-CSIC. Campus UIB, 07122 Palma de Mallorca, Spain*

We study the effect that the heterogeneity present among the elements of an ensemble of coupled excitable neurons have on the collective response of the system to an external signal. We have considered two different interaction scenarios, one in which the neurons are diffusively coupled and another in which the neurons interact via pulse-like signals. We found that the type of interaction between the neurons has a crucial role in determining the response of the system to the external modulation. We develop a mean-field theory based on an order parameter expansion that quantitatively reproduces the numerical results in the case of diffusive coupling.

## I. INTRODUCTION

Synchronized behavior arising among the constituents of an ensemble is common in nature. Examples include the synchronized flashing of fireflies, the blossoming of flowers, cardiac cells giving rise to the pacemaker role of the sinoatrial node of the heart and the electrical pulses of neurons. This global behavior can originate from a common response to an external stimulus or might appear in autonomous, non-forced, systems. The theoretical basis for the understanding of synchronization in non-forced systems was put forward by Winfree ([17]) who showed that the interaction –i.e. coupling– between the constituents is an essential ingredient for the existence of a synchronized output. The seminal work on coupled oscillators by Kuramoto ([7]) offered a model case whose solution confirms the basic hypothesis of Winfree: while interaction helps towards the achievement of a common behavior, a perfect order can be achieved only in the absence of diversity –heterogeneity– among the components of an ensemble. In the Kuramoto model, diversity manifests when the oscillators have different natural frequencies, those they display when uncoupled from each other. While this result holds for systems that can be described

by coupled oscillators, recent results indicate that in other cases diversity among the constituents might actually have a positive role in the setting of a resonant behavior with an external signal. This was first demonstrated in ([14]) and has been since extended to many other systems ([1, 2, 5, 9, 10, 13, 16, 16, 18, 19, 19]). In the case of non-forced excitable systems, a unifying treatment of the role of noise and diversity has been developed in [15].

Many biological systems, including neurons, display excitability as a response to an external perturbation. Excitability is characterized by the existence of a threshold, a largely independent response to a suprathreshold input and a refractory time. It is well established that the dynamical features of neurons can be described by excitable models: when a neuron is perturbed by a single impulse, the neuron can generate a single spike, and when perturbed by a continuum signal, a train of spikes with a characteristic firing frequency can appear instead. Although the creation and propagation of electrical signals has been thoroughly studied by physiologists for at least a century, the most important landmark in this field is due to Hodgkin and Huxley ([6]), who developed the first quantitative model to describe the evolution of the membrane potential in the squid giant axon. Because of the central importance of cellular electrical activity in biological systems and because this model forms the basis for the study of excitable systems, it remains to this date an important model for analysis. Subsequently a simplified version of this model, known as the FitzHugh-Nagumo (FHN) model ([3]), that captures many of the qualitative features of the Hodgkin-Huxley model was developed. The FHN model has two variables, one fast and one slow. The fast variable represents the evolution of the membrane potential and it is known as the excitation variable. The slow variable accounts for the  $K^+$  ionic current and is known as the recovery variable. One virtue of this model is that it can be studied using phase-plane methods, because it is a two variable system. For instance, the fast variable has a cubic nullcline while the slow variable has a linear nullcline and the study of both nullclines and their intersections allow to determine the different dynamical regimes of the model. The FHN model can then be extended by coupling the individual elements, and provides an interesting model, for example, of coupled neuron populations.

In the initial studies of the dynamics of the FHN and similar models, the individual units (e.g. neurons) were treated as identical. However, it is evident that real populations of neurons display a large degree of variability, both in morphology and dynamical activity; that is, there is a diversity in the population of these biological units. Then, it is natural to ask what role diversity plays in the global dynamical behavior of these systems and a lot of activity has been developed along these lines in the recent years. In general, it has been found, as noted above, that diversity can in fact

be an important parameter in controlling the dynamics. In particular, it has been shown that both excitable and bistable systems can improve their response to an external stimulus if there is an adequate degree of diversity in the constituent units ([14]).

In this paper we continue our study of the effect of diversity, investigating in some depth its role in the FHN model of excitable systems. We consider in detail a system of many neurons coupled either chemically or electrically. We show that in both cases a right amount of diversity can indeed enhance the response to a periodic external stimulus and we discuss in detail the difference between the two types of coupling. The outline of the paper is as follows: In section II we present the FHN model and the coupling schemes considered. Next, in section III we present the main results we have obtained from numerical simulations. Afterwards, in section IV we develop an approximate theoretical treatment based on an order parameter expansion which allows us to obtain a quantitative description of the behavior of the model and compare its predictions with the numerical results. Finally, in section V we summarize the conclusions.

## II. FITZHUGH-NAGUMO MODEL

### A. Dynamical equations

Let us consider a system of excitable neurons described by the FHN model. The dynamical equations describing the activity of a single neuron are:

$$\epsilon \frac{dx}{dt} = x(1-x)(x-b) - y + d, \quad (1)$$

$$\frac{dy}{dt} = x - cy + a, \quad (2)$$

where  $x(t)$  and  $y(t)$  represent, respectively, the fast membrane potential and the slow potassium gating variable of a neuron. We assume that the time scales of these variables are well separated by the small parameter  $\epsilon = 0.01$ . Other parameters are fixed to  $b = 0.5$ ,  $c = 4.6$  and  $d = 0.1$  ([4]), while the value of  $a$  will fluctuate from one neuron to the other, so reflecting the intrinsic diversity in the neuronal ensemble.

Let us concentrate first on the dynamics of a single neuron as described by Eqs. (1)-(2). This dynamics has a strong dependence on the parameter  $a$ . Three different operating regimes are identify: for  $a \lesssim -0.09$  the system has a stable focus in the right branch of the cubic nullcline leading the system to an excitable regime; for  $-0.09 \lesssim a \lesssim 0.01$  a limit cycle around an unstable

focus appears (oscillatory regime) and for  $0.01 \lesssim a$  a stable focus appears again, now at the left side of the cubic nullcline (excitable regime). Figure 1 (a) shows the nullclines  $f(x) = x(1-x)(x-b) + d$  and  $g(x, a) = (x+a)/c$  of the system in the three operating regimes described above, for  $a = -0.1, 0.0$  and  $0.06$ , respectively. In the excitable regime, spikes (also known as pulses), can appear as a result of an external perturbation of large enough amplitude. A convenient definition is that a spike appears when the membrane potential of the neuron exceeds a certain threshold value, e.g.  $x \geq 0.5$ . In the oscillatory regime, spikes appear spontaneously with an intrinsic firing frequency  $\nu$  which, as shown in Figure 1 (b), does not depend much on the value of  $a$ .

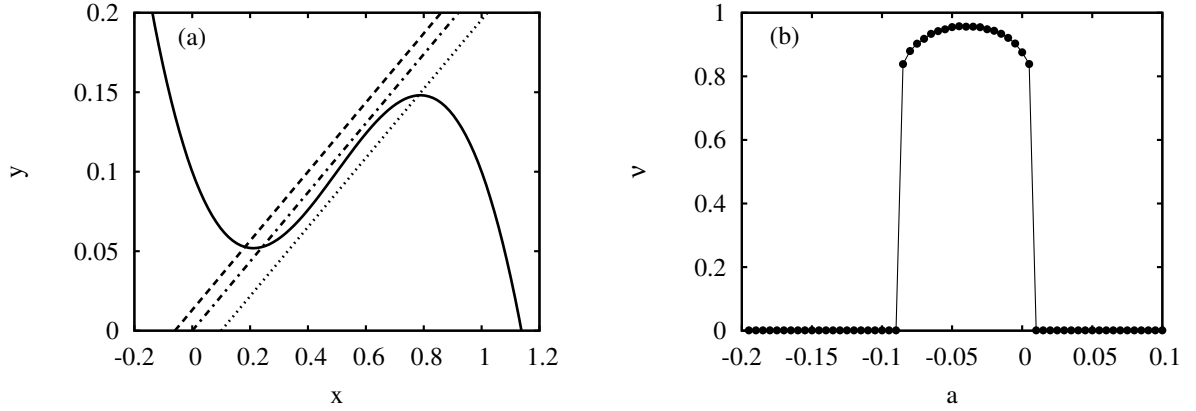


FIG. 1: (a) Nullclines of the FHN system for three different values of the parameter  $a$ .  $f(x)$  (solid line) and  $g(x, a)$  for  $a = -0.1$  (dotted line);  $a = 0.0$  (dash-dotted line) and  $a = 0.06$  (dashed line). (b) Dependence of the firing frequency  $\nu$  on  $a$ .

To illustrate the dynamical behavior of  $x(t)$  and  $y(t)$ , we show in Figure 2 the phase-portrait for three different values of  $a = -0.1, 0.0$  and  $0.06$  corresponding to the three nullclines represented in Figure 1 (a).

### B. Coupling scenarios: electrical versus chemical interaction

We consider now that we have an ensemble of  $N$  coupled neurons. Each one is described by dynamical variables  $x_i(t)$ ,  $y_i(t)$ ,  $i = 1, \dots, N$ , obeying the FitzHugh-Nagumo equations. The neurons are not isolated from each other, but interact mutually. The full set of equations is now:

$$\epsilon \frac{dx_i}{dt} = x_i(1-x_i)(x_i-b) - y_i + d + I_i^{syn}(t), \quad (3)$$

$$\frac{dy_i}{dt} = x_i - cy_i + a_i, \quad (4)$$

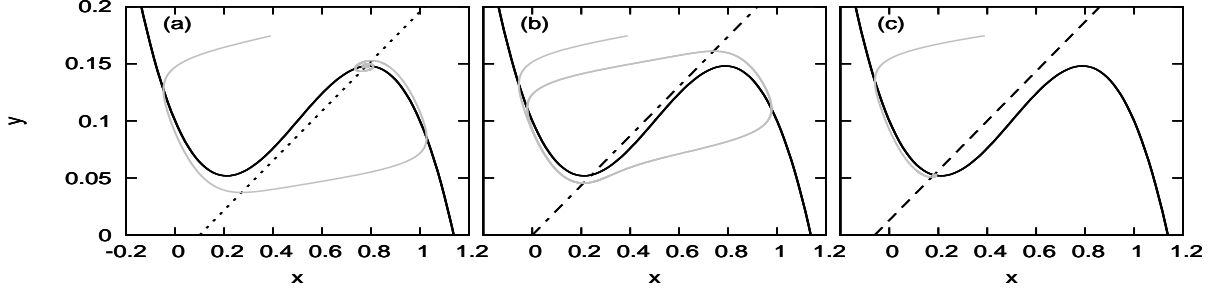


FIG. 2: Phase-space portrait of the FHN system for different values of  $a$ . Gray line represents the evolution of  $\{x, y\}$ .  $f(x)$  (black line) and  $g(x, a)$  for (a)  $a = -0.1$  dotted line (excitable regime); (b)  $a = 0.0$  dash-dotted line (oscillatory regime) and (c)  $a = 0.06$  dash line (excitable regime).

where  $I_i^{syn}(t)$  is the coupling term accounting for all the interactions of neuron  $i$  with other neurons. To take into account the natural diversity of the units, we assume that the parameter  $a_i$ , that controls the degree of excitability of the neuron, varies from neuron to neuron. In particular we assign to  $a_i$  random values following a Gaussian distribution with mean  $\langle a_i \rangle = a$  and correlations  $\langle (a_i - a)(a_j - a) \rangle = \delta_{ij}\sigma^2$ . We use  $\sigma$  as a measure of the heterogeneity of the system and, in the following, we use the value of  $\sigma$  as an indicator of the degree of diversity. If  $\sigma = 0$ , all neurons have exactly the same set of parameters, while large values of  $\sigma$  indicate a large dispersion in the dynamical properties of individual neurons.

The most common way of communication between neurons is via chemical synapses, where the transmission is carried by an agent called neurotransmitter. In these synapses, neurons are separated by a synaptic cleft and the neurotransmitter has to diffuse to reach the post-synaptic receptors. In the chemical coupling case the synaptic current is modeled as:

$$I_i^{syn}(t) = \frac{K}{N_c} \sum_{j=1}^{N_c} g_{ij} r_j(t) (E_i^s - x_i). \quad (5)$$

In this configuration, we consider that neuron  $i$  is connected to  $N_c$  neurons randomly chosen from the set of  $N - 1$  available neurons. Once a connection is established between neuron  $i$  and  $j$ , we assume that the reciprocal connection is also created. Then, the connection fraction of each neuron is defined as  $f = N_c/(N - 1)$ . In Eq. (5)  $K$  determines the coupling strength and  $g_{ij}$  represents the maximum conductance in the synapse between the neurons  $i$  and  $j$ . For simplicity, we limit our study to the homogeneous coupling configuration, where  $g_{ij} = 1$  if neurons  $i$  and  $j$  are connected and  $g_{ij} = 0$  otherwise. The character of the synapse is determined by the synaptic reversal potential of the receptor neuron,  $E_i^s$ . An excitatory (resp. inhibitory) synapse is characterized by a value

of  $E_i^s$  greater (resp. smaller) than the membrane resting potential. We consider  $E_i^s = 0.7$  for the excitatory synapses and  $E_i^s = -2.0$  for the inhibitory ones. We also define the fraction of excitatory neurons (those that project excitatory synapses) in the system as  $f_e = N_e/N$  being  $N_e$  the number of excitatory neurons.

Finally,  $r_j(t)$  is a time dependent function representing the fraction of bound receptors and it is given by:

$$r_j(t) = \begin{cases} 1 - e^{-\alpha t} & \text{for } t \leq t_{on}, \\ (1 - e^{-\alpha t_{on}}) e^{-\beta(t-t_{on})} & \text{for } t > t_{on} \end{cases} \quad (6)$$

where  $\alpha = 2.5$  and  $\beta = 3.5$  are the rise and decay time constants, respectively. Here  $t_{on} = 0.1$  represents the time the synaptic connection remains active and  $t$  is the time from the spike generation in the presynaptic neuron.

There is another type of synapse where the membranes of the neurons are in close contact and thus the transmission of the signal is achieved directly (electrical synapses). In this case of electrically-mediated interactions, also known as diffusive coupling, the total synaptic current is proportional to the sum of the membrane potential difference between a neuron and its neighbors, and it is given by:

$$I_i^{syn}(t) = \frac{K}{N_c} \sum_{j=1}^{N_c} (x_j - x_i). \quad (7)$$

The last ingredient of our model is the presence of an external forcing that acts upon all neurons simultaneously. Although our results are very general, for the sake of concreteness we use a periodic forcing of amplitude  $A$  and period  $T$ . More precisely, the dynamical equations under the presence of this forcing are modified as:

$$\epsilon \frac{dx_i}{dt} = x_i(1 - x_i)(x_i - b) - y_i + d + I_i^{syn}(t), \quad (8)$$

$$\frac{dy_i}{dt} = x_i - cy_i + a_i + A \sin\left(\frac{2\pi}{T}t\right), \quad (9)$$

which is the basis of our subsequent analysis.

### III. RESULTS

We are interested in analysing the response of the global system to the external forcing. We will show that its effect can be enhanced under the presence of the right amount of diversity in the

set of parameters  $a_i$ , i.e. a conveniently defined response will reach its maximum amplitude at an intermediate value of the root mean square value  $\sigma$ .

In order to quantify the global response of the system with respect to the diversity, we use the spectral amplification factor defined as

$$\eta = \frac{4}{A^2} \left| \left\langle e^{-i\frac{2\pi}{T}t} X(t) \right\rangle \right|^2. \quad (10)$$

where  $X(t) = \frac{1}{N} \sum_{i=1}^N x_i(t)$  is the global, average collective variable of the system and  $\langle \cdot \rangle$  denotes a time average. We will analyze separately the cases of electrical and chemical coupling.

### 1. Electrical coupling

In this subsection we concentrate on the situation in which the neurons are electrically (diffusively) coupled in a random network, where a neuron  $i$  is connected randomly with  $N_c = f(N - 1)$  other neurons. The mean value of the Gaussian distribution of the parameters  $a_i$  is fixed to  $a = 0.06$  and the coupling strength to  $K = 0.6$ . Figure 3 shows the spectral amplification factor  $\eta$  as a function of the diversity  $\sigma$  for fixed values of the amplitude  $A = 0.05$  and two different values of the period  $T$  of the external forcing, for an increasing connection fraction  $f$ . It can be seen from Figure 3 that intermediate values of  $\sigma$  give a maximum response in the spectral amplification factor. Moreover, the maximum value shifts slightly to smaller values of  $\sigma$  as the fraction of connected neurons  $f$  increases. We have also observed that a period  $T$  of the external forcing close to the inverse of the intrinsic firing frequency of the neurons ( $\nu \approx 0.9$ , according to Figure 1b) yields the largest response.

In order to further illustrate the response of the system to the external sinusoidal modulation, Figure 4 shows the raster plot of the ensemble (lower panels) and the time traces of ten randomly chosen neurons (upper panels) for different values of the diversity parameter. It can be seen in both the top and bottom panels of this figure that an intermediate level of diversity gives a more regular behavior than either smaller or larger values of  $\sigma$ . This fact is more evident in the time traces where the amplitude of the oscillation varies randomly for large  $\sigma$  values.

### 2. Chemical coupling

We consider in this subsection the situation in which the units are chemically coupled. Figure 5 shows the spectral amplification factor  $\eta$  as a function of the diversity  $\sigma$  for fixed values of the

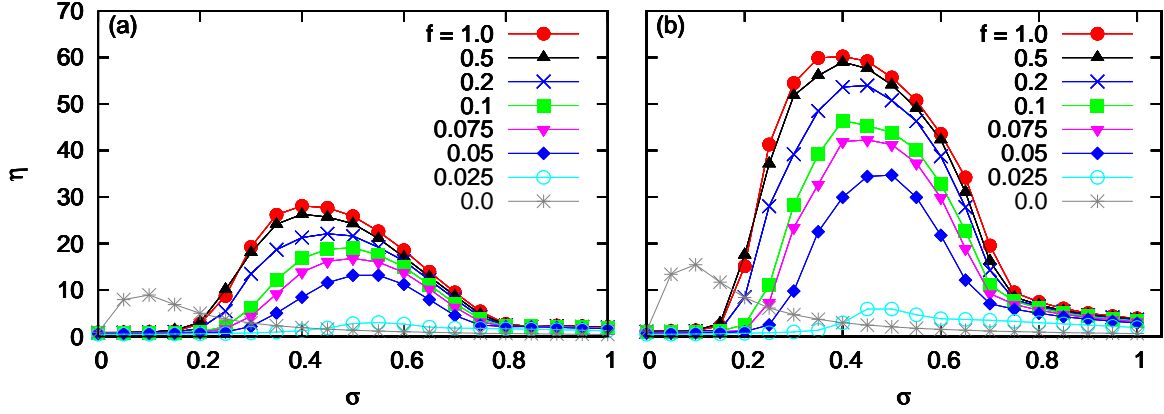


FIG. 3: Spectral amplification factor  $\eta$  as a function of  $\sigma$  for an increasing fraction of connected neurons  $f$  for two different periods of the external modulation. (a)  $T = 1.6$  and (b)  $T = 1.11$ . Other parameters:  $a = 0.06$ ,  $K = 0.6$  and  $A = 0.05$ .

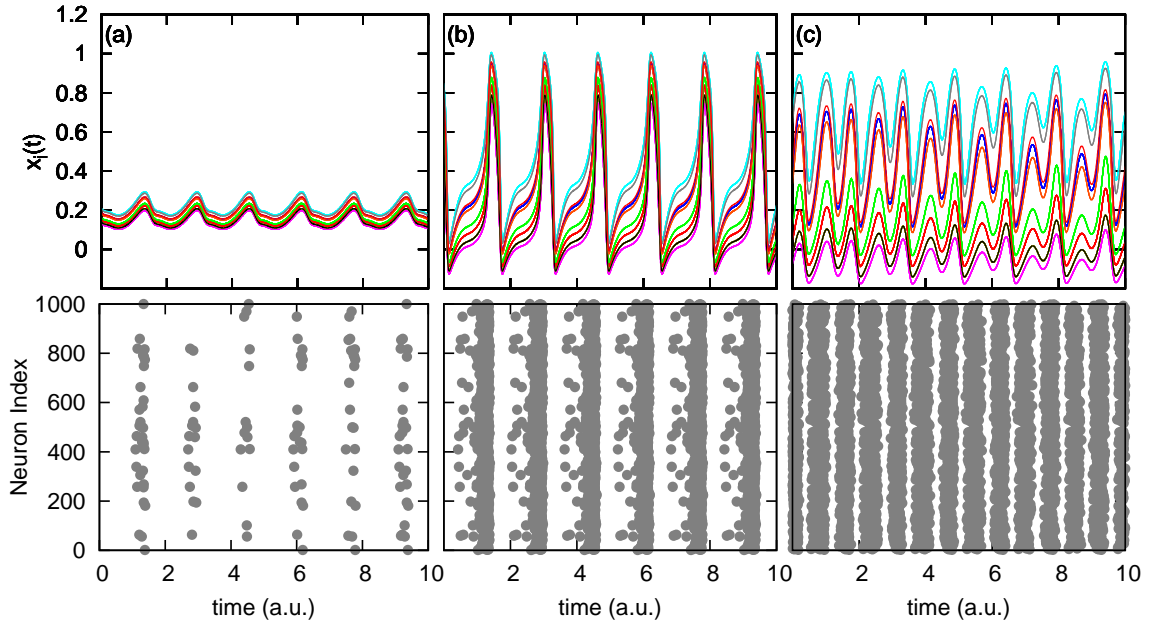


FIG. 4: Time traces of ten randomly chosen neurons and raster plot (every time a neuron spikes a dot is drawn) of the fully connected,  $f = 1$ , ensemble in the case of electrical coupling for three different values of the diversity parameter: (a)  $\sigma = 0.1$ , (b)  $\sigma = 0.4$  and (c)  $\sigma = 0.9$ . Other parameters:  $a = 0.06$ ,  $K = 0.6$ ,  $A = 0.05$  and  $T = 1.6$ .

amplitude  $A = 0.05$  and two different periods of the external modulation when the fraction of randomly connected neurons  $f$  increases. The coupling strength is fixed to  $K = 1.5$ . The fraction



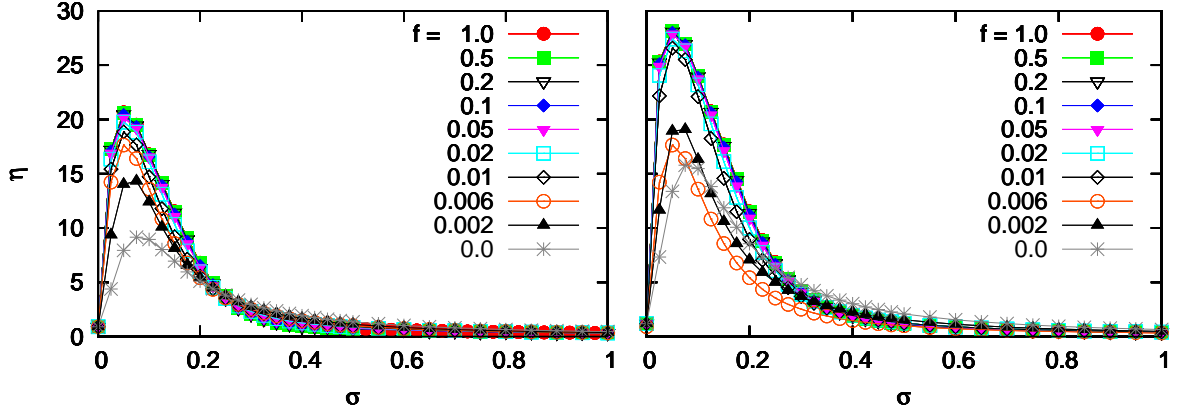


FIG. 5: Spectral amplification factor  $\eta$  as a function of  $\sigma$  for an increasing fraction of connected neurons  $f$ . The fraction of excitatory neurons was fixed to  $f_e = 0.8$ . Two different periods of the external modulation have been considered: (a)  $T = 1.6$  and (b)  $T = 1.11$ .

of excitatory neurons in the system is set to  $f_e = 0.8$ . It can be seen from Figure 5 that the spectral amplification factor  $\eta$  increases as  $f$  increases, reaching the maximum response at  $f \simeq 0.05$ . Interestingly, beyond this value  $\eta$  does not change significantly, indicating that the response of the system does not improve when the percentage of connected neurons is larger than 5%. Or, put in another way, with a 5% connectivity, the system already behaves as being fully connected as far as the response to the external forcing is concerned. It is also worth noting that the maximum response is always at the same value of  $\sigma$ , independent of  $f$ . The effect of changing the ratio of excitatory/inhibitory synapses in our system is shown in Figure 6 in the globally coupled case  $f = 1$ . The spectral amplification factor increases as the fraction of excitatory connections  $f_e$  increases, while the position of the maximum shifts slightly to larger values of  $\sigma \simeq 0.05$ .

Comparing the results from both electrical and chemical coupling schemes, it can be seen that the electrical coupling gives a larger value of  $\eta$  but requires, at the same time, a larger diversity. The electrical coupling also exhibits a larger range of diversity values for which the system has an optimal response compared with the chemical coupling. In contrast, the optimal response in the chemical coupling scheme occurs for small values of the diversity and does not significantly change in amplitude and width when the percentage of connected neurons  $f$  is increased above 5%.

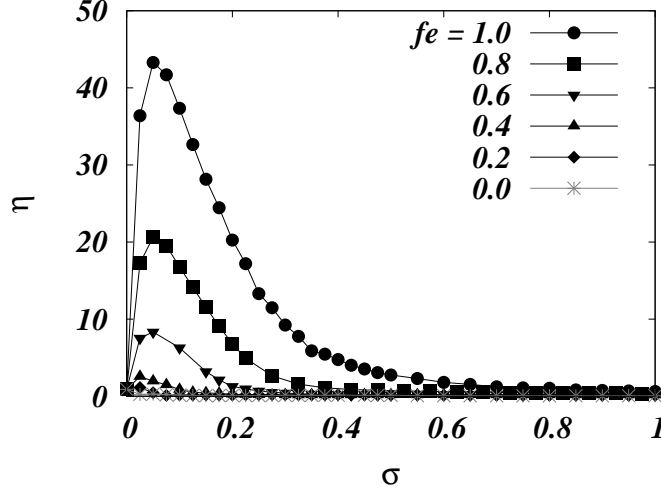


FIG. 6: Spectral amplification factor  $\eta$  as a function of  $\sigma$  for an increasing fraction of excitatory synapses  $f_e$  in the case that neurons are globally coupled,  $f = 1$ . Other parameters:  $a = 0.06$ ,  $K = 1.5$ ,  $A = 0.05$  and  $T = 1.6$ .

#### IV. ORDER PARAMETER EXPANSION

It is possible to perform an approximate analysis of the effect of the diversity in the case of diffusive (electrical) coupling. The analysis allows to gain insight into the amplification mechanism by showing how the effective nullclines of the global variable  $X(t)$  are modified when varying  $\sigma$ . The theoretical analysis is based upon a modification of the so-called order parameter expansion developed by Monte and D'Ovidio ([11, 12]) along the lines of [8]. The approximation begins by expanding the dynamical variables around their average values  $X(t) = \frac{1}{N} \sum_i x_i$  and  $Y(t) = \frac{1}{N} \sum_i y_i$  as  $x_j(t) = X(t) + \delta_j^x(t)$ ,  $y_j(t) = Y(t) + \delta_j^y(t)$  and the diversity parameter around its mean value  $a_j = a + \delta_j^a$ . The validity of this expansion relies on the existence of a coherent behavior by which the individual units  $x_j$  deviate in a small amount  $\delta_j^x$  from the global behavior characterized by the global average variable  $X(t)$ . It also assumes that the deviations  $\delta_j^a$  are small. We expand equations (8) for  $\frac{dx_i}{dt}$  and (9) for  $\frac{dy_i}{dt}$  up to second order in  $\delta_i^x$ ,  $\delta_i^y$  and  $\delta_i^a$ ; the resulting equations are:

$$\epsilon \frac{dx_i}{dt} = f(X, Y) + f_x(X, Y) \delta_i^x + f_y(X, Y) \delta_i^y + \frac{1}{2} f_{xx}(X, Y) (\delta_i^x)^2, \quad (11)$$

$$\frac{dy_i}{dt} = g(X, Y, a) + g_x(X, Y, a) \delta_i^x + g_a(X, Y, a) \delta_i^a, \quad (12)$$

where

$$\begin{aligned} f(x, y) &= x(1-x)(x-b) - y + d - Kx, \\ g(x, y, a) &= x - cy + a + A \sin\left(\frac{2\pi}{T}t\right), \end{aligned} \quad (13)$$

and we used the notation  $f_x$  to indicate the derivative of  $f$  with respect to  $x$  and so forth. Note that Eq. (12) is exact since it is linear in all the variables. If we average Eq. (11)-(12) using  $\langle \cdot \rangle = \frac{1}{N} \sum_i \cdot$  we obtain:

$$\epsilon \frac{dX}{dt} = f(X, Y) + \frac{1}{2} f_{xx}(X, Y) \Omega^x, \quad (14)$$

$$\frac{dY}{dt} = g(X, Y, a), \quad (15)$$

where we have used  $\langle \delta_j^x \rangle = \langle \delta_j^y \rangle = \langle \delta_j^a \rangle = 0$  and defined the second moment  $\Omega^x = \langle (\delta_j^x)^2 \rangle$ . We also defined  $\Omega^y = \langle (\delta_j^y)^2 \rangle$ ,  $\sigma^2 = \langle (\delta_j^a)^2 \rangle$ , and the shape factors  $\Sigma^{xy} = \langle \delta_j^x \delta_j^y \rangle$ ,  $\Sigma^{xa} = \langle \delta_j^x \delta_j^a \rangle$  and  $\Sigma^{ya} = \langle \delta_j^y \delta_j^a \rangle$ . The evolution equations for the second moments are found from the first-order expansion  $\dot{\delta}_j^x = \dot{x}_j - \dot{X}$ , so that  $\dot{\Omega}^x = 2\langle \delta_j^x \dot{\delta}_j^x \rangle$  and  $\dot{\Sigma}^{xy} = \langle \dot{\delta}_j^x \delta_j^y + \delta_j^x \dot{\delta}_j^y \rangle$ , where the dot stands for time derivative.

$$\epsilon \dot{\delta}_i^x = f_x \delta_i^x + f_y \delta_i^y + \frac{1}{2} f_{xx} [(\delta_i^x)^2 - \Omega^x], \quad (16)$$

$$\dot{\delta}_i^y = g_x \delta_i^x + g_y \delta_i^y + g_a \delta_i^a, \quad (17)$$

$$\dot{\Omega}^x = \frac{2}{\epsilon} [f_x \Omega^x + f_y \Sigma^{xy}], \quad (18)$$

$$\dot{\Omega}^y = 2 [g_x \Sigma^{xy} + g_y \Omega^y + g_a \Sigma^{ya}], \quad (19)$$

$$\dot{\Sigma}^{xy} = \frac{1}{\epsilon} [f_x \Sigma^{xy} + f_y \Omega^y] + g_x \Omega^x + g_y \Sigma^{xy} + g_a \Sigma^{xa}, \quad (20)$$

$$\dot{\Sigma}^{xa} = \frac{1}{\epsilon} [f_x \Sigma^{xa} + f_y \Sigma^{ya}], \quad (21)$$

$$\dot{\Sigma}^{ya} = g_x \Sigma^{xa} + g_y \Sigma^{ya} + g_a \sigma^2. \quad (22)$$

The system of Eq. (14)-(15) together with Eq. (18)-(22) forms a closed set of differential equations for the average collective variables  $X(t)$  and  $Y(t)$ :

$$\epsilon \dot{X} = -X^3 + (1+b)X^2 - (b+3\Omega^x)X + (1+b)\Omega^x + d - Y, \quad (23)$$

$$\dot{Y} = X - cY + a + A \sin\left(\frac{2\pi}{T}t\right), \quad (24)$$

$$\epsilon \dot{\Omega}^x = 2(-3X^2 + 2(1+b)X - b - K)\Omega^x - 2\Sigma^{xy}, \quad (25)$$

$$\dot{\Omega}^y = 2[\Sigma^{xy} - c\Omega^y + \Sigma^{ya}], \quad (26)$$

$$\dot{\Sigma}^{xy} = \frac{1}{\epsilon} [(-3X^2 + 2(1+b)X - b - K)\Sigma^{xy} - \Omega^y]$$

$$+ \Omega^x - c\Sigma^{xy} + \Sigma^{xa}, \quad (27)$$

$$\epsilon \dot{\Sigma}^{xa} = (-3X^2 + 2(1+b)X - b - K)\Sigma^{xa} - \Sigma^{ya}, \quad (28)$$

$$\dot{\Sigma}^{ya} = \Sigma^{xa} - c\Sigma^{ya} + \sigma^2. \quad (29)$$

Numerical integration of this system allows us to obtain  $X(t)$ , from which we can compute the spectral amplification factor  $\eta$ . The value of  $\eta$  obtained from the expansion is later compared with that obtained from the numerical integration of the Eqs. (8)-(4) (see Figure 9 below).

We can obtain another set of closed equations for  $X(t)$  and  $Y(t)$  if we perform an adiabatic elimination of the fluctuations, i.e.,  $\dot{\Omega}^x = \dot{\Omega}^y = \dot{\Sigma}^{xy} = \dot{\Sigma}^{xa} = \dot{\Sigma}^{ya} = 0$ , yielding to:

$$\begin{aligned} \Sigma^{xa} &= \frac{\sigma^2}{cH(x)-1}, & \Sigma^{ya} &= \frac{H(x)\sigma^2}{cH(x)-1}, & \Sigma^{xy} &= \frac{H(x)\sigma^2}{(cH(x)-1)^2}, \\ \Omega^x &= \frac{\sigma^2}{(cH(x)-1)^2}, & \Omega^y &= \frac{H^2(x)\sigma^2}{(cH(x)-1)^2}, \end{aligned} \quad (30)$$

with  $H(x) = -3x^2 + 2(1+b)x - b - K$ . Substituting  $\Omega^x$  in Eqs. (23)-(24), we find a closed form for the equations describing the evolution of the mean-field variables  $X(t)$  and  $Y(t)$ :

$$\epsilon \dot{X} = -X^3 + (1+b)X^2 - \left[ b + \frac{3\sigma^2}{(cH(X)-1)^2} \right] X + \frac{(1+b)\sigma^2}{(cH(X)-1)^2} + d - Y, \quad (31)$$

$$\dot{Y} = X - cY + a + A \sin\left(\frac{2\pi}{T}t\right) \quad (32)$$

These equations provide a closed form for the nullclines of the global variables  $X$  and  $Y$  for the non-forcing case  $A = 0$ . They also reflect how diversity influences these variables. Figure 7 shows these nullclines  $Y_1(X, \sigma)$  and  $Y_2(X, a)$  of Eqs. (31)-(32) respectively for  $a = 0.06$  and different values of the diversity  $\sigma$ . It can be seen in the figure that the diversity changes the shape of the cubic nullcline  $Y_1(X, \sigma)$  leading to a loss of stability of the fixed point of the system that, for a certain range of  $\sigma$ , becomes a limit cycle. To schematize the behavior of the global variables  $X$  and  $Y$  when the diversity changes, we show in Figure 8 the phase-portrait for different values of  $\sigma = 0.0, 0.5, 0.8, 1.0, 1.2$  and  $1.4$  (corresponding to the values represented in Figure 7). It can be seen that there is a range of  $\sigma$  for which the system exhibits a collective oscillatory behavior even in the absence of the weak external modulation.

With the collective variable  $X(t)$  obtained from the adiabatic elimination we can estimate the spectral amplification factor  $\eta$ . Figure 9 shows the results obtained from the numerical integration of Eqs. (23)-(29), together with the numerical simulation of the full system, Eqs. (8)-(4) and the adiabatic approximation obtained from Eqs. (31) and (32). It can be seen that our order parameter

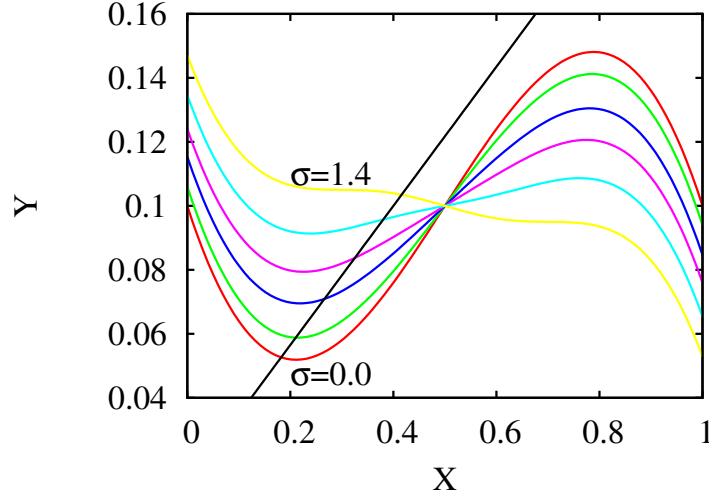


FIG. 7: Nullclines of Eq. (31)-(32) for different values of the diversity  $\sigma$ .  $Y_1(X, \sigma)$  for  $\sigma$ : (a) 0.0 (red line), (b) 0.5 (green line), (c) 0.8 (blue line), (d) 1.0 (violet line), (e) 1.2 (cyan line) and (f) 1.4 (yellow line). The nullcline  $Y_2(X, a)$  of Eq. (32) for  $a = 0.06$  is represented with a black line.

expansion is in good agreement with the numerical integration of the full system, even in the case in which the second moments are adiabatically eliminated.

## V. CONCLUSIONS

We have studied the effect of the diversity in an ensemble of coupled neurons described by the FHN model. We have observed that an intermediate value of diversity can enhance the response of the system to an external periodic forcing. We have studied both electrical and chemical coupling schemes finding that the electrical coupling induces a larger response of the system to an external weak modulation, as well as existing for a wider range. In contrast, the chemical coupling scheme exhibits a smaller optimal amplitude and narrower range of response, however, for smaller values of the diversity. We have also found that the response of the system in the electrical coupling scheme strongly depends on the fraction of connected neurons in the system whereas it does not improve much above a small fraction of connected neurons in the chemical coupling scheme. We have also developed an order parameter expansion whose results are in good agreement with those obtained numerically for the electrically (diffusively) coupled FHN system. By an adiabatic elimination of the fluctuations we have found a closed form of the effective nullclines of the global

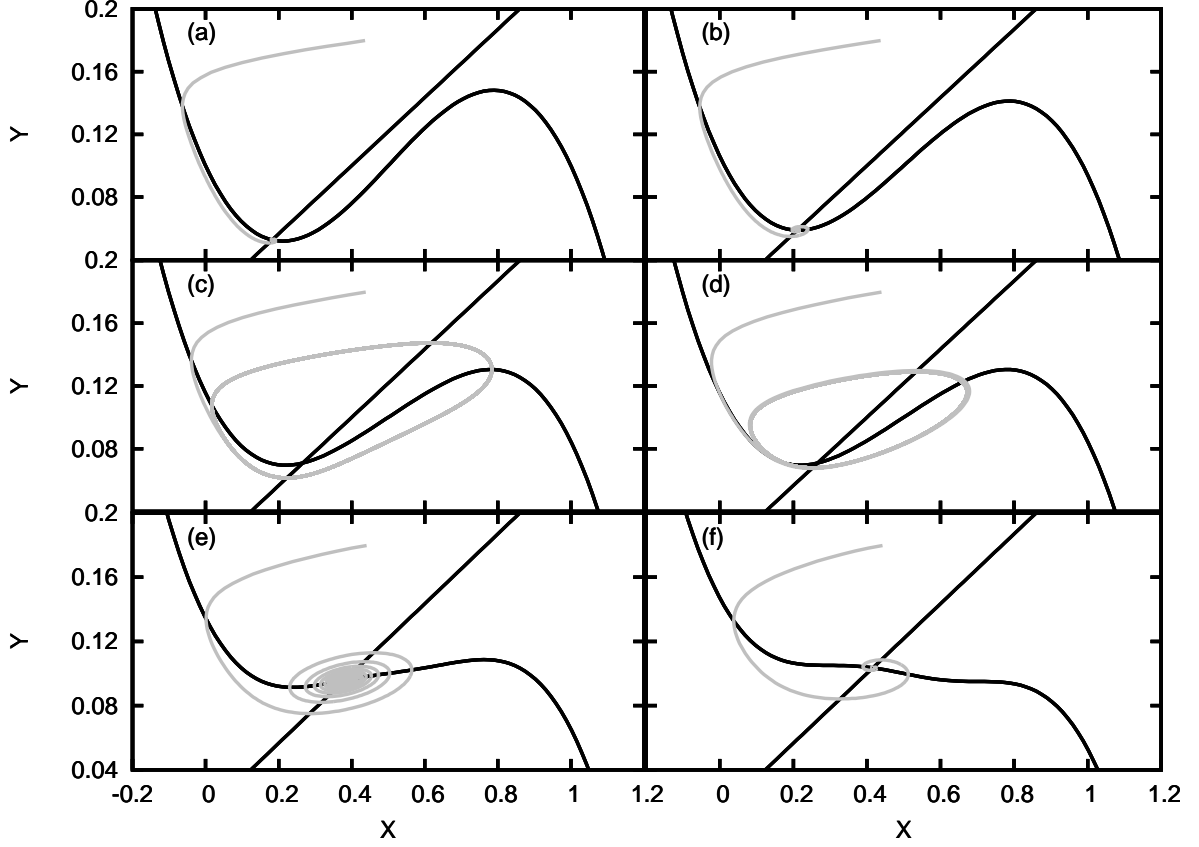


FIG. 8: Phase-space portrait for different values of  $\sigma$ . Grey line represents the evolution of  $\{X, Y\}$ . The black lines represent the nullcline  $Y_2(X, a)$  for  $a = 0.06$  and the cubic nullcline  $Y_1(X, \sigma)$  for  $\sigma$ : (a) 0.0, (b) 0.5, (c) 0.8, (d) 1.0, (e) 1.2 and (f) 1.4.

collective variables of the system obtaining a simple expression of how the diversity influences the collective variables of the system.

The microscopic mechanism leading the system to a resonant behavior with the external signal is as follows: in the homogeneous situation, where all the units are identical, the weak external modulation cannot induce any spike in the system. When the diversity increases, a fraction of the neurons enters into the oscillatory regime and, due to the interactions, pull the other neurons with them. This leads the system to an oscillatory collective behavior that follows the external signal. For larger values of the diversity, the fraction of neurons in the oscillatory regime decreases and the rest of neurons offer some resistance to being pulled by the oscillatory ones; thus, the system cannot respond to the external signal anymore. These results suggest that the diversity present in biological systems may have an important role in enhancing the response of the system to the detection of weak signals.

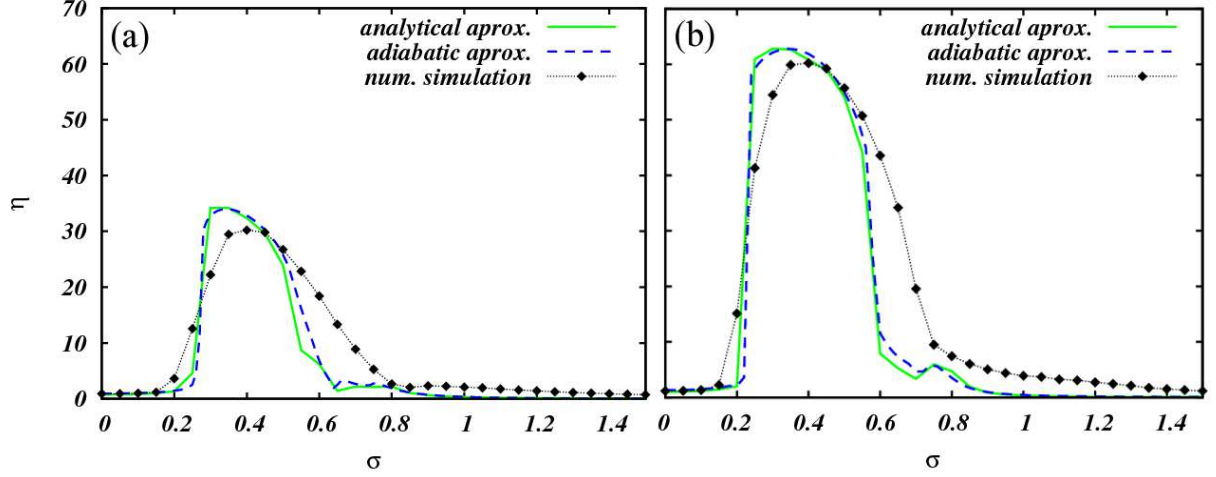


FIG. 9: Order parameter expansion versus numerical integration of the full system. An adiabatic approximation is also included (see text). Two different periods of the external modulation have been considered: (a)  $T = 1.6$  and (b)  $T = 1.11$ . Other parameter as in Figure 3.

We acknowledge financial support from the following organizations: National Science Foundation (Grant DMR- 0702890); G. Harold and Leila Y. Mathers Foundation; European Commission Project GABA (FP6-NEST Contract 043309); EU NoE Biosim (LSHB-CT-2004-005137); and MEC (Spain) and Feder (project FIS2007-60327).

- 
- [1] J.A. Acebron, S. Lozano, and A. Arenas. Amplified signal response in scale-free networks by collaborative signaling. *Phys. Rev. Lett.*, 99:128701, 2007.
  - [2] H.S. Chen, Y. Shen, and Z.H. Hou. Resonant response of forced complex networks: The role of topological disorder. *Chaos*, 19:033122, 2009.
  - [3] R. FitzHugh. Impulses and physiological states in theoretical models of nerve membrane. *Biophysical J.*, 1:445, 1961.
  - [4] E. Glatt, M. Gassel, and F. Kaiser. Noise-induced synchronisation in heterogeneous nets of neural elements. *Europhys. Lett.*, 81:40004, 2008.
  - [5] M. Gosak. Cellular diversity promotes intercellular  $\text{Ca}^{2+}$  wave propagation. *Biophysical Chemistry*, 139:53, 2009.
  - [6] A. L. Hodgkin and A. Huxley. A quantitative description of membrane current and it applications to conduction and excitation in nerve. *J. Physiol.*, 117:500, 1952.

- [7] Y. Kuramoto. International symposium on mathematical problems in theoretical physics. In H. Araki, editor, *Lectures notes in Physics No 30*. Springer, New York, 1975.
- [8] N.Komin and R. Toral. Phase transitions induced by microscopic disorder: a study based on the order parameter expansion. *ArXiv*:1003.1061.
- [9] M. Perc, M. Gosak, and S. Kralj. Stochastic resonance in soft matter systems: combined effects of static and dynamic disorder. *Soft Matter*, 4:1861, 2008.
- [10] S. Postnova, K. Voigt, and H.A. Braun. A mathematical model of homeostatic regulation of sleep-wake cycles by hypocretin/orexin. *J. of Biological Rhythms*, 24:523, 2009.
- [11] S.D.Monte and F.D'Ovidio. Dynamics of order parameters for globally coupled oscillators. *Europhys. Lett.*, 58:21, 2002.
- [12] S.D.Monte, F.D'Ovidio, H. Chaté, and E. Mosekilde. Effects of microscopic disorder on the collective dynamics of globally coupled maps. *Physica D*, 205:25, 2005.
- [13] C.J. Tessone and R. Toral. Diversity-induced resonance in a model for opinion formation. *European Physical Journal B*, 71:549, 2009.
- [14] C.J. Tessone, C.R. Mirasso, R. Toral, and J.D. Gunton. Diversity-induced resonance. *Phys. Rev. Lett.*, 97:194101, 2006.
- [15] C.J. Tessone, A. Scire, R. Toral, and P. Colet. Theory of collective ring induced by noise or diversity in excitable media. *Phys. Rev. E*, 75:016203, 2007.
- [16] E. Ullner, J. Buceta, A. Diez-Noguera, and J. Garcia-Ojalvo. Noise-induced coherence in multicellular circadian clocks. *Biophysical Journal*, 96:3573, 2009.
- [17] A.T. Winfree. Biological rhythms and the behavior of populations of coupled oscillators. *J. Theoret. Biol.*, 16:15, 1967.
- [18] D. Wu, S.Q. Zhu, and X.Q. Luo. Cooperative effects of random time delays and small-world topologies on diversity-induced resonance. *Europhys. Letters*, 86:50002, 2009.
- [19] D. Zanette. Interplay of noise and coupling in heterogeneous ensembles of phase oscillators. *European Physical Journal B*, 69:269, 2009.